B_K for 2+1 flavour domain wall fermions from 24^3 and $32^3 \times 64$ lattices

Chris Kelly

University of Edinburgh
RBC & UKQCD Collaborations

Mon 14^{th} July

Outline

The neutral kaon mixing amplitude B_K

Outline

The neutral kaon mixing amplitude B_K

Ensemble details

Outline

The neutral kaon mixing amplitude B_K

Ensemble details

Measurement of B_K

Outline

The neutral kaon mixing amplitude B_K

Ensemble details

Measurement of B_K

The chiral extrapolation of B_K

Outline

The neutral kaon mixing amplitude B_K

Ensemble details

Measurement of B_K

The chiral extrapolation of B_K

The non-perturbative renormalisation of B_K

Outline

- The neutral kaon mixing amplitude B_K
- Ensemble details
- Measurement of B_K
- The chiral extrapolation of B_K
- The non-perturbative renormalisation of B_K
- Conclusions and Outlook

The neutral kaon mixing amplitude B_K

Kaon mixing

- Indirect CP violation in neutral kaon sector

Kaon mixing

- Indirect CP violation in neutral kaon sector
- Neutral kaon mixing amplitude:

Kaon mixing

- Indirect CP violation in neutral kaon sector
- Neutral kaon mixing amplitude:

$$A(K^0 \to \bar{K}^0) = \frac{G_F}{2} \sum_i V^i_{\mathrm{CKM}} C_i(\mu) \langle K^0 | Q_i(\mu) | \bar{K}^0 \rangle$$

Kaon mixing

- Indirect CP violation in neutral kaon sector
- Neutral kaon mixing amplitude:

$$A(K^0 \to \bar{K}^0) = \frac{G_F}{2} \sum_i V^i_{\mathrm{CKM}} C_i(\mu) \langle K^0 | Q_i(\mu) | \bar{K}^0 \rangle$$

scheme dependent
perturbative factor
summarising
contributions from
scales $\gg \mu$

Kaon mixing

- Indirect CP violation in neutral kaon sector
- Neutral kaon mixing amplitude:

$$A(K^0 \to \bar{K}^0) = \frac{G_F}{2} \sum_i V^i_{\mathrm{CKM}} C_i(\mu) \overbrace{\langle K^0 | Q_i(\mu) | \bar{K}^0 \rangle}^{\text{scheme dependent hadronic matrix element at scale } \mu \sim M_K \text{ obtainable from lattice}}$$

scheme dependent perturbative factor summarising contributions from scales $\gg \mu$

B_K

- B_K parameterises the matrix element of the four-quark $K^0 \rightarrow \bar{K}^0$ operator

B_K

- B_K parameterises the matrix element of the four-quark $K^0 \to \bar{K}^0$ operator

$$B_K \equiv \frac{\langle K^0 | \mathcal{O}_{VV+AA} | \bar{K}^0 \rangle}{\frac{8}{3} f_K^2 M_K^2}$$

B_K

- B_K parameterises the matrix element of the four-quark $K^0 \to \bar{K}^0$ operator

$$B_K \equiv \frac{\langle K^0 | \mathcal{O}_{VV+AA} | \bar{K}^0 \rangle}{\frac{8}{3} f_K^2 M_K^2}$$

$$\mathcal{O}_{VV+AA} = (\bar{s}\gamma_\mu d)(\bar{s}\gamma_\mu d) + (\bar{s}\gamma_5\gamma_\mu d)(\bar{s}\gamma_5\gamma_\mu d)$$

B_K

- B_K parameterises the matrix element of the four-quark $K^0 \to \bar{K}^0$ operator

$$B_K \equiv \frac{\langle K^0 | \mathcal{O}_{VV+AA} | \bar{K}^0 \rangle}{\frac{8}{3} f_K^2 M_K^2}$$

$$\mathcal{O}_{VV+AA} = (\bar{s}\gamma_\mu d)(\bar{s}\gamma_\mu d) + (\bar{s}\gamma_5\gamma_\mu d)(\bar{s}\gamma_5\gamma_\mu d)$$

- B_K related to measure of indirect CP violation $\epsilon_K = \frac{K_L \to (\pi\pi)}{K_S \to (\pi\pi)}$
  $\to$relation contains unknown *direct* CP violating parameters.

B_K

- B_K parameterises the matrix element of the four-quark $K^0 \to \bar{K}^0$ operator

$$B_K \equiv \frac{\langle K^0 | \mathcal{O}_{VV+AA} | \bar{K}^0 \rangle}{\frac{8}{3} f_K^2 M_K^2}$$

$$\mathcal{O}_{VV+AA} = (\bar{s}\gamma_\mu d)(\bar{s}\gamma_\mu d) + (\bar{s}\gamma_5\gamma_\mu d)(\bar{s}\gamma_5\gamma_\mu d)$$

- B_K related to measure of indirect CP violation $\epsilon_K = \frac{K_L \to (\pi\pi)}{K_S \to (\pi\pi)}$ $\to$relation contains unknown *direct* CP violating parameters.
- ϵ_K known experimentally to high precision $\Rightarrow$ B_K constrains unknown direct CP violating parameters.

Ensemble details

Details of ensembles

$\mathbf{24^3 \times 64}$

$\mathbf{32^3 \times 64}$

Details of ensembles

$24^3 \times 64$

- 2+1f domain wall fermion ensemble with $L_s = 16$

$32^3 \times 64$

- 2+1f domain wall fermion ensemble with $L_s = 16$

Details of ensembles

$24^3 \times 64$

- 2+1f domain wall fermion ensemble with $L_s = 16$
- Iwasaki gauge action $\beta = 2.13$

$32^3 \times 64$

- 2+1f domain wall fermion ensemble with $L_s = 16$

Details of ensembles

$24^3 \times 64$

- 2+1f domain wall fermion ensemble with $L_s = 16$
- Iwasaki gauge action $\beta = 2.13$

$32^3 \times 64$

- 2+1f domain wall fermion ensemble with $L_s = 16$
- Iwasaki gauge action $\beta = 2.25$

Details of ensembles

$24^3 \times 64$

- 2+1f domain wall fermion ensemble with $L_s = 16$
- Iwasaki gauge action $\beta = 2.13$
- $a^{-1} = 1.729(28)$ GeV $\rightarrow$ $(2.74\,\mathrm{fm})^3$ lattice volume

$32^3 \times 64$

- 2+1f domain wall fermion ensemble with $L_s = 16$
- Iwasaki gauge action $\beta = 2.25$

Details of ensembles

$24^3 \times 64$

- 2+1f domain wall fermion ensemble with $L_s = 16$
- Iwasaki gauge action $\beta = 2.13$
- $a^{-1} = 1.729(28)$ GeV $\rightarrow$ $(2.74\,\mathrm{fm})^3$ lattice volume

$32^3 \times 64$

- 2+1f domain wall fermion ensemble with $L_s = 16$
- Iwasaki gauge action $\beta = 2.25$
- $a^{-1} = 2.42(4)\frac{0.47}{r_0\,(\mathrm{fm})}$ GeV $\rightarrow$ $(2.61\,\mathrm{fm})^3$ lattice volume

Details of ensembles

$24^3 \times 64$

- 2+1f domain wall fermion ensemble with $L_s = 16$
- Iwasaki gauge action $\beta = 2.13$
- $a^{-1} = 1.729(28)$ GeV $\rightarrow$ $(2.74\,\mathrm{fm})^3$ lattice volume
- Strange sea quark mass 0.04 lattice units

$32^3 \times 64$

- 2+1f domain wall fermion ensemble with $L_s = 16$
- Iwasaki gauge action $\beta = 2.25$
- $a^{-1} = 2.42(4)\frac{0.47}{r_0\,(\mathrm{fm})}$ GeV $\rightarrow$ $(2.61\,\mathrm{fm})^3$ lattice volume

Details of ensembles

$24^3 \times 64$

- 2+1f domain wall fermion ensemble with $L_s = 16$
- Iwasaki gauge action $\beta = 2.13$
- $a^{-1} = 1.729(28)$ GeV $\rightarrow$ $(2.74\,\mathrm{fm})^3$ lattice volume
- Strange sea quark mass 0.04 lattice units

$32^3 \times 64$

- 2+1f domain wall fermion ensemble with $L_s = 16$
- Iwasaki gauge action $\beta = 2.25$
- $a^{-1} = 2.42(4)\frac{0.47}{r_0\,(\mathrm{fm})}$ GeV $\rightarrow$ $(2.61\,\mathrm{fm})^3$ lattice volume
- Strange sea quark mass 0.03 lattice units

Up/down sea quark masses

$24^3 \times 64$

latt. units	m_π (MeV)
0.03	626
0.02	558
0.01	345
0.005	331

$32^3 \times 64$

latt. units	m_π (MeV)
0.008	$\sim$ 420
0.006	$\sim$ 360
0.004	$\sim$ 300

Highly preliminary data as datasets only partially complete

Measurement of B_K

Method comparison

$\mathbf{24^3 \times 64}$

$\mathbf{32^3 \times 64}$

Method comparison

$24^3 \times 64$

- 2 gauge-fixed wall sources at $t = 5$, 59 for propagators

$32^3 \times 64$

Method comparison

$24^3 \times 64$

- 2 gauge-fixed wall sources at $t = 5, 59$ for propagators
- Use $p + a$ boundary conditions $\longrightarrow$ removes unwanted round-the-world contributions.

$32^3 \times 64$

Method comparison

$24^3 \times 64$

- 2 gauge-fixed wall sources at $t = 5, 59$ for propagators
- Use $p + a$ boundary conditions $\rightarrow$ removes unwanted round-the-world contributions.
- Costs 4 inversions per configuration.

$32^3 \times 64$

Method comparison

$24^3 \times 64$

- 2 gauge-fixed wall sources at $t = 5, 59$ for propagators
- Use $p + a$ boundary conditions $\rightarrow$ removes unwanted round-the-world contributions.
- Costs 4 inversions per configuration.

$32^3 \times 64$

- 1 gauge-fixed wall source at $t = 0$

Method comparison

$24^3 \times 64$

- 2 gauge-fixed wall sources at $t = 5, 59$ for propagators
- Use $p + a$ boundary conditions $\rightarrow$ removes unwanted round-the-world contributions.
- Costs 4 inversions per configuration.

$32^3 \times 64$

- 1 gauge-fixed wall source at $t = 0$
- Use $p + a$ and $p - a$ boundary conditions $\rightarrow$ gives forwards and backwards propagating quarks.

Method comparison

$24^3 \times 64$

- 2 gauge-fixed wall sources at $t = 5, 59$ for propagators
- Use $p + a$ boundary conditions $\rightarrow$ removes unwanted round-the-world contributions.
- Costs 4 inversions per configuration.

$32^3 \times 64$

- 1 gauge-fixed wall source at $t = 0$
- Use $p + a$ and $p - a$ boundary conditions $\rightarrow$ gives forwards and backwards propagating quarks.
- Costs 2 inversions per configuration.

B_K example plateaux

$24^3 \times 64 \; m_l = 0.005$

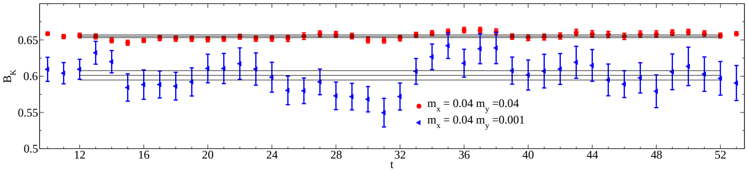

Preliminary $32^3 \times 64 \; m_l = 0.004$

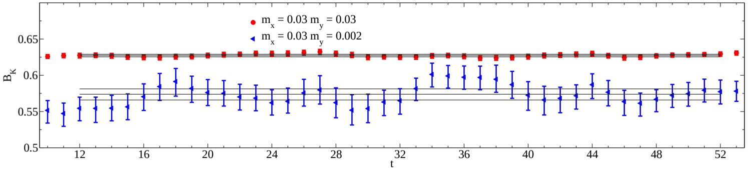

The chiral extrapolation of B_K

B_K chiral fit forms

- We use NLO $SU(2) \times SU(2)$ partially-quenched chiral perturbation theory (PQChPT) for maximum use of ensembles.

B_K chiral fit forms

- We use NLO $SU(2) \times SU(2)$ partially-quenched chiral perturbation theory (PQChPT) for maximum use of ensembles.
- Kaon sector is coupled to $SU(2)$ soft pion loops at lowest order in non-relativistic expansion

B_K chiral fit forms

- We use NLO $SU(2) \times SU(2)$ partially-quenched chiral perturbation theory (PQChPT) for maximum use of ensembles.
- Kaon sector is coupled to $SU(2)$ soft pion loops at lowest order in non-relativistic expansion
  $\longrightarrow$ direct connection to HMχPT

B_K chiral fit forms

- We use NLO $SU(2) \times SU(2)$ partially-quenched chiral perturbation theory (PQChPT) for maximum use of ensembles.
- Kaon sector is coupled to $SU(2)$ soft pion loops at lowest order in non-relativistic expansion
  $\longrightarrow$ direct connection to HMχPT
- 24^3 analysis [Allton *et al* arXiv:0804.0473] indicated $SU(3) \times SU(3)$ PQChPT has large higher order corrections and doesn't fit data well up to physical strange quark mass (R. Mawhinney).

$SU(2) \times SU(2)$ PQChPT fit form for B_K

$$B_K = B_K^0 \Big[\; 1 + \frac{2B(m_d + m_{\rm res})c_0}{f^2} + \frac{2B(m_y + m_{\rm res})c_1}{f^2} - \frac{2B(m_y + m_{\rm res})}{32\pi^2 f^2} \log\left(\frac{2B(m_y + m_{\rm res})}{\Lambda_\chi^2}\right) \Big]$$

$SU(2) \times SU(2)$ PQChPT fit form for B_K

$$B_K = B_K^0 \Big[\quad 1 + \frac{2B(m_d + m_{\rm res})c_0}{f^2} + \frac{2B(m_y + m_{\rm res})c_1}{f^2} - \frac{2B(m_y + m_{\rm res})}{32\pi^2 f^2} \log\left(\frac{2B(m_y + m_{\rm res})}{\Lambda_\chi^2}\right) \Big]$$

- 5 free parameters:

$SU(2) \times SU(2)$ PQChPT fit form for B_K

$$
\begin{aligned}
B_K &= B_K^0 \Big[\quad 1 + \frac{2B(m_d+m_{\rm res})c_0}{f^2} + \frac{2B(m_y+m_{\rm res})c_1}{f^2} \\
&\qquad - \frac{2B(m_y+m_{\rm res})}{32\pi^2 f^2} \log\left(\frac{2B(m_y+m_{\rm res})}{\Lambda_\chi^2}\right) \Big]
\end{aligned}
$$

- 5 free parameters: B_K^0, B, f, c_0, c_1

$SU(2) \times SU(2)$ PQChPT fit form for B_K

$$
\begin{aligned}
B_K &= B_K^0 \Big[\quad 1 + \frac{2B(m_d+m_{\rm res})c_0}{f^2} + \frac{2B(m_y+m_{\rm res})c_1}{f^2} \\
&\qquad - \frac{2B(m_y+m_{\rm res})}{32\pi^2 f^2} \log\left(\frac{2B(m_y+m_{\rm res})}{\Lambda_\chi^2}\right) \; \Big]
\end{aligned}
$$

- 5 free parameters: B_K^0, B, f, c_0, c_1

$SU(2) \times SU(2)$ PQChPT fit form for B_K

$$
\begin{aligned}
B_K &= B_K^0 \Big[\quad 1 + \frac{2B(m_d + m_{\rm res}) c_0}{f^2} + \frac{2B(m_y + m_{\rm res}) c_1}{f^2} \\
&\qquad - \frac{2B(m_y + m_{\rm res})}{32\pi^2 f^2} \log\left(\frac{2B(m_y + m_{\rm res})}{\Lambda_\chi^2} \right) \Big]
\end{aligned}
$$

- 5 free parameters: B_K^0, B, f, c_0, c_1

$SU(2) \times SU(2)$ PQChPT fit form for B_K

$$B_K = B_K^0 \left[1 + \frac{2B(m_d + m_{\rm res}) c_0}{f^2} + \frac{2B(m_y + m_{\rm res}) c_1}{f^2} - \frac{2B(m_y + m_{\rm res})}{32\pi^2 f^2} \log\left(\frac{2B(m_y + m_{\rm res})}{\Lambda_\chi^2}\right) \right]$$

- 5 free parameters: B_K^0, B, f, c_0, c_1

$SU(2) \times SU(2)$ PQChPT fit form for B_K

$$
\begin{aligned}
B_K &= B_K^0 \Big[\quad 1 + \frac{2B(m_d + m_{\mathrm{res}})c_0}{f^2} + \frac{2B(m_y + m_{\mathrm{res}})c_1}{f^2} \\
&\qquad - \frac{2B(m_y + m_{\mathrm{res}})}{32\pi^2 f^2} \log\left(\frac{2B(m_y + m_{\mathrm{res}})}{\Lambda_\chi^2}\right) \Big]
\end{aligned}
$$

- 5 free parameters: B_K^0, B, f, c_0, c_1

$SU(2) \times SU(2)$ PQChPT fit form for B_K

$$B_K = B_K^0 \Big[1 + \frac{2B(m_d+m_{\rm res})c_0}{f^2} + \frac{2B(m_y+m_{\rm res})c_1}{f^2} - \frac{2B(m_y+m_{\rm res})}{32\pi^2 f^2} \log\left(\frac{2B(m_y+m_{\rm res})}{\Lambda_\chi^2}\right) \Big]$$

- 5 free parameters: B_K^0, B, f, c_0, c_1
- Use simultaneous pure $SU(2) \times SU(2)$ PQChPT fit (no coupling to Kaon sector) to $F_{\rm PS}$ and $M_{\rm PS}$ to determine B and f (E. Scholz)

$SU(2) \times SU(2)$ PQChPT fit form for B_K

$$B_K = B_K^0 \Big[\quad 1 + \frac{2B(m_d + m_{\mathrm{res}})c_0}{f^2} + \frac{2B(m_y + m_{\mathrm{res}})c_1}{f^2}$$
$$- \frac{2B(m_y + m_{\mathrm{res}})}{32\pi^2 f^2} \log\left(\frac{2B(m_y + m_{\mathrm{res}})}{\Lambda_\chi^2}\right) \Big]$$

- 5 free parameters: B_K^0, B, f, c_0, c_1
- Use simultaneous pure $SU(2) \times SU(2)$ PQChPT fit (no coupling to Kaon sector) to F_{PS} and M_{PS} to determine B and f (E. Scholz)

$\rightarrow$ perform frozen 3-parameter fit to B_K

Simultaneous PQChPT fits to $F_{\rm PS}$ and $M_{\rm PS}$: $f_{\rm PS}$

$24^3 \times 64$

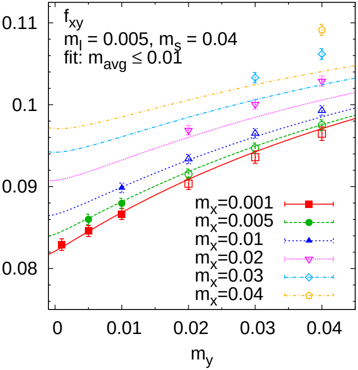

$32^3 \times 64$

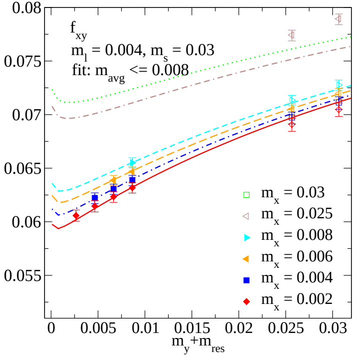

Simultaneous PQChPT fits to F_{PS} and M_{PS} : f_{PS}

- For fixed m_l chiral fit forms non-analytic as $m_{x/y} \longrightarrow 0$

$32^3 \times 64$

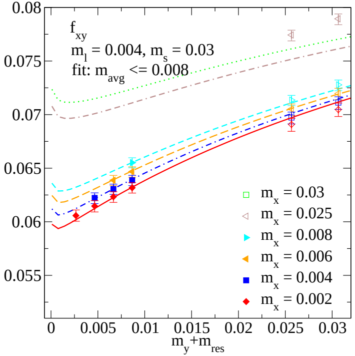

Simultaneous PQChPT fits to F_{PS} and M_{PS} : f_{PS}

- For fixed m_l chiral fit forms non-analytic as $m_{x/y} \to 0$
- Perform full PQChPT fit to all data points then extrapolate to chiral limit along *unitary* curve $m_x = m_y = m_l \to 0$ to obtain physical f_{PS}.

$32^3 \times 64$

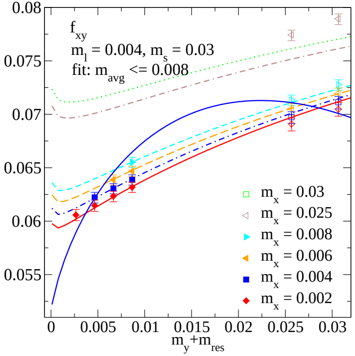

Simultaneous PQChPT fits to F_{PS} and M_{PS} : f_{PS}

- For fixed m_l chiral fit forms non-analytic as $m_{x/y} \to 0$
- Perform full PQChPT fit to all data points then extrapolate to chiral limit along *unitary* curve $m_x = m_y = m_l \to 0$ to obtain physical f_{PS}.
- Unitary curve is finite valued at chiral limit.

$32^3 \times 64$

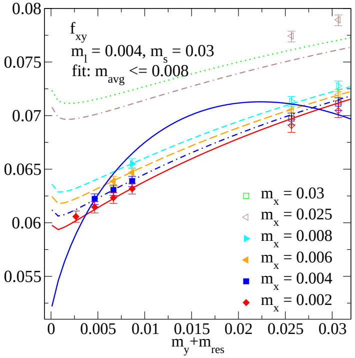

Simultaneous PQChPT fits to F_{PS} and M_{PS} : M_{PS}

$24^3 \times 64$

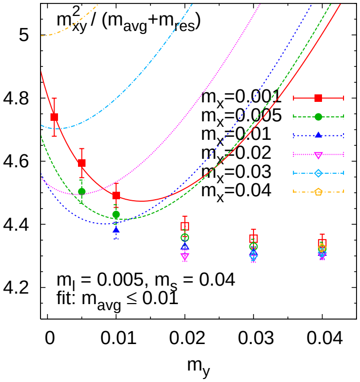

$32^3 \times 64$

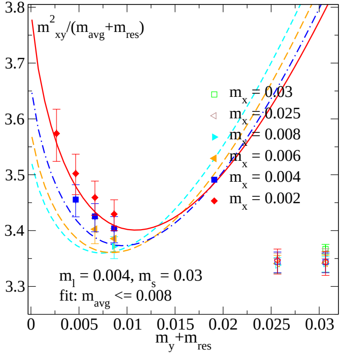

PQChPT fits to B_K

$24^3 \times 64$

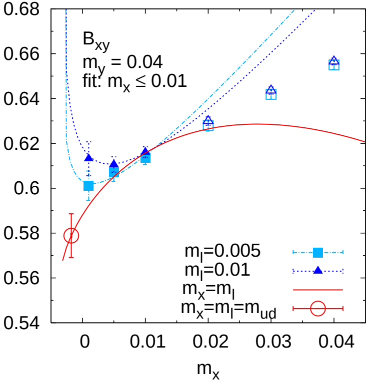

$32^3 \times 64$

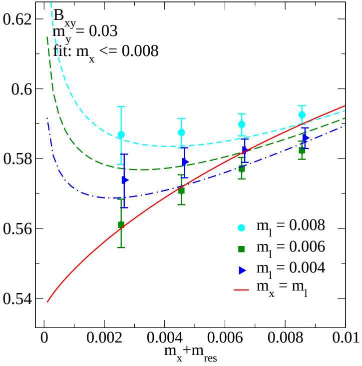

- Unitary curve is fixed m_s, $m_x = m_l \rightarrow m_l^{\text{phys}}$

PQChPT fits to B_K

$24^3 \times 64$

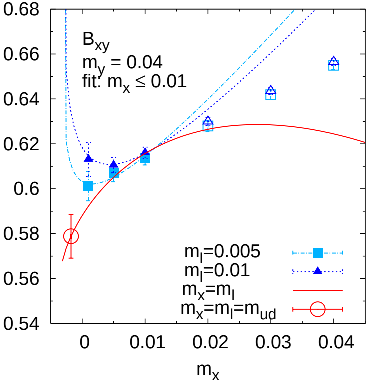

$32^3 \times 64$

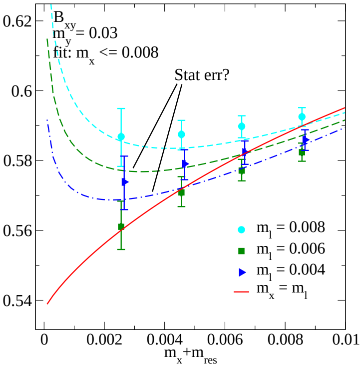

- Unitary curve is fixed m_s, $m_x = m_l \to m_l^{\rm phys}$

$24^3 \times 64$ B_K chiral limit results – Allton *et al* [arXiv:0804.0473]

- $24^3 \times 64$ $B_K^{lat} = 0.565(10)$.

$24^3 \times 64$ B_K chiral limit results – Allton *et al* [arXiv:0804.0473]

- $24^3 \times 64$ $B_K^{lat} = 0.565(10)$.
- $32^3 \times 64$ extrapolation not yet available, dataset only partially complete
  – Stat uncertainties in data sets, unknown physical quark masses

The non-perturbative renormalisation of B_K

Why NPR?

- Lattice perturbative (DWF) calculations exist but:

Why NPR?

- Lattice perturbative (DWF) calculations exist but:
  - exist only at low order

Why NPR?

- Lattice perturbative (DWF) calculations exist but:
  - exist only at low order
  - are poorly convergent

Why NPR?

- Lattice perturbative (DWF) calculations exist but:
  - exist only at low order
  - are poorly convergent
  - involve prescription dependent ambiguities such as MF improvement

Why NPR?

- Lattice perturbative (DWF) calculations exist but:
  - exist only at low order
  - are poorly convergent
  - involve prescription dependent ambiguities such as MF improvement
- Use Rome-Southampton RI/MOM scheme

Bilinear vertices

- $Z_V = Z_A$ due to good chiral symmetry

Bilinear vertices

- $Z_V = Z_A$ due to good chiral symmetry
- At high momenta, $\Lambda_A = \Lambda_V = \frac{Z_q}{Z_A} = \frac{Z_q}{Z_V}$ should hold.

Bilinear vertices

- $Z_V = Z_A$ due to good chiral symmetry
- At high momenta, $\Lambda_A = \Lambda_V = \frac{Z_q}{Z_A} = \frac{Z_q}{Z_V}$ should hold.
- Therefore can use Λ_A *or* Λ_V as a measure of $\frac{Z_q}{Z_A}$.

Bilinear vertices

- $Z_V = Z_A$ due to good chiral symmetry
- At high momenta, $\Lambda_A = \Lambda_V = \frac{Z_q}{Z_A} = \frac{Z_q}{Z_V}$ should hold.
- Therefore can use Λ_A *or* Λ_V as a measure of $\frac{Z_q}{Z_A}$.
- Λ_A and Λ_V expected to differ at low momenta due to QCD spontaneous chiral symmetry breaking.

Bilinear vertices

- $Z_V = Z_A$ due to good chiral symmetry
- At high momenta, $\Lambda_A = \Lambda_V = \frac{Z_q}{Z_A} = \frac{Z_q}{Z_V}$ should hold.
- Therefore can use Λ_A *or* Λ_V as a measure of $\frac{Z_q}{Z_A}$.
- Λ_A and Λ_V expected to differ at low momenta due to QCD spontaneous chiral symmetry breaking.
- However, even at high momenta we find $\Lambda_A \neq \Lambda_V$ at 2% level

Bilinear vertices

- $Z_V = Z_A$ due to good chiral symmetry
- At high momenta, $\Lambda_A = \Lambda_V = \frac{Z_q}{Z_A} = \frac{Z_q}{Z_V}$ should hold.
- Therefore can use Λ_A *or* Λ_V as a measure of $\frac{Z_q}{Z_A}$.
- Λ_A and Λ_V expected to differ at low momenta due to QCD spontaneous chiral symmetry breaking.
- However, even at high momenta we find $\Lambda_A \neq \Lambda_V$ at 2% level $\longrightarrow$ difference caused by kinematic choice : Exceptional momentum configuration

Bilinear vertices

- $Z_V = Z_A$ due to good chiral symmetry
- At high momenta, $\Lambda_A = \Lambda_V = \frac{Z_q}{Z_A} = \frac{Z_q}{Z_V}$ should hold.
- Therefore can use Λ_A *or* Λ_V as a measure of $\frac{Z_q}{Z_A}$.
- Λ_A and Λ_V expected to differ at low momenta due to QCD spontaneous chiral symmetry breaking.
- However, even at high momenta we find $\Lambda_A \neq \Lambda_V$ at 2% level
  $\longrightarrow$ difference caused by kinematic choice : Exceptional momentum configuration
  $\longrightarrow$ Gives weak $1/p^2$ suppression of low energy chiral symmetry breaking.

Chiral symmetry breaking and exceptional momenta

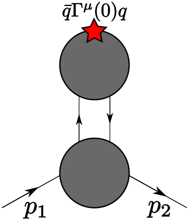

- Generic bilinear vertex graph

Chiral symmetry breaking and exceptional momenta

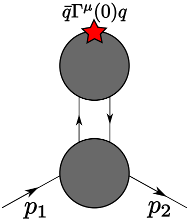

- Generic bilinear vertex graph
- $p^2 \to \infty$ behaviour governed by subgraph with least negative degree of divergence through which we can route all **hard** external momenta.

Chiral symmetry breaking and exceptional momenta

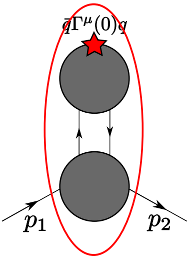

- Generic bilinear vertex graph
- $p^2 \to \infty$ behaviour governed by subgraph with least negative degree of divergence through which we can route all **hard** external momenta.
- For $p_1 \neq p_2$ this is the entire graph.

Chiral symmetry breaking and exceptional momenta

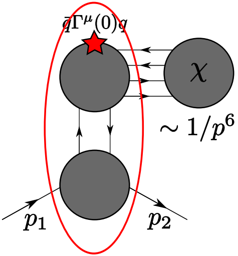

- Generic bilinear vertex graph
- $p^2 \to \infty$ behaviour governed by subgraph with least negative degree of divergence through which we can route all **hard** external momenta.
- For $p_1 \neq p_2$ this is the entire graph.
- Can connect to **low-energy** subgraphs which are affected by spont. chiral symmetry breaking, but:

Chiral symmetry breaking and exceptional momenta

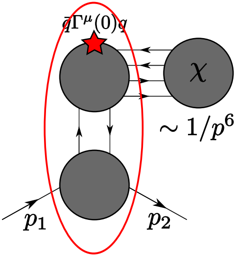

- Generic bilinear vertex graph
- $p^2 \to \infty$ behaviour governed by subgraph with least negative degree of divergence through which we can route all **hard** external momenta.
- For $p_1 \neq p_2$ this is the entire graph.
- Can connect to **low-energy** subgraphs which are affected by spont. chiral symmetry breaking, but:

  $\rightarrow$ Low energy subgraph not contained within circled subgraph

Chiral symmetry breaking and exceptional momenta

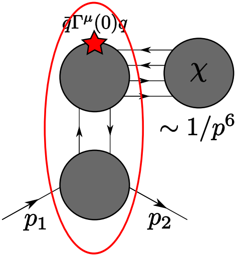

- Generic bilinear vertex graph
- $p^2 \to \infty$ behaviour governed by subgraph with least negative degree of divergence through which we can route all **hard** external momenta.
- For $p_1 \neq p_2$ this is the entire graph.
- Can connect to **low-energy** subgraphs which are affected by spont. chiral symmetry breaking, but:
  $\longrightarrow$ Low energy subgraph not contained within circled subgraph
  $\longrightarrow$ Adding extra external legs to circled subgraph increases suppression of the graph

Chiral symmetry breaking and exceptional momenta

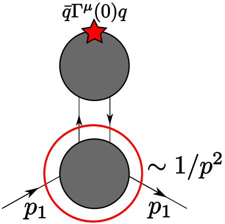

- However in case $p_2 - p_1 = 0$ then high momenta do not enter internal subgraphs

Chiral symmetry breaking and exceptional momenta

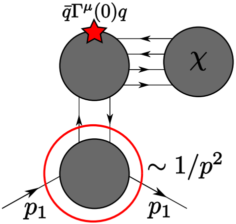

- However in case $p_2 - p_1 = 0$ then high momenta do not enter internal subgraphs
- Graph free to couple to low-energy chiral symmetry breaking subgraphs with no further suppression

Chiral symmetry breaking and exceptional momenta

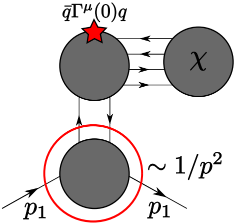

- However in case $p_2 - p_1 = 0$ then high momenta do not enter internal subgraphs
- Graph free to couple to low-energy chiral symmetry breaking subgraphs with no further suppression
- This is an exceptional momentum configuration

Chiral symmetry breaking and exceptional momenta

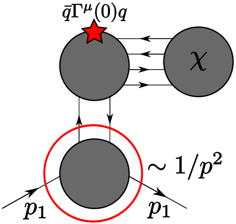

- However in case $p_2 - p_1 = 0$ then high momenta do not enter internal subgraphs
- Graph free to couple to low-energy chiral symmetry breaking subgraphs with no further suppression
- This is an exceptional momentum configuration
- Chiral symmetry breaking induces difference between Λ_A and Λ_V $\rightarrow$ use $\frac{1}{2}(\Lambda_A + \Lambda_V) \approx \frac{Z_q}{Z_A}$

B_K NPR with RI/MOM and exceptional momenta

- Calculate four-quark vertex matrix element in Landau gauge.

B_K NPR with RI/MOM and exceptional momenta

- Calculate four-quark vertex matrix element in Landau gauge.
- Amputate vertex with ensemble averaged unrenormalised propagator, giving $\Lambda_{\mathcal{O}_{VV+AA}}$

B_K NPR with RI/MOM and exceptional momenta

- Calculate four-quark vertex matrix element in Landau gauge.
- Amputate vertex with ensemble averaged unrenormalised propagator, giving $\Lambda_{\mathcal{O}_{VV+AA}}$
- Renormalisation condition: Fix to tree level value at $\mu^2 = p^2$

$$\frac{Z_{VV+AA}}{Z_q^2}\Lambda_{\mathcal{O}_{VV+AA}} = \mathcal{O}^{\text{tree}}_{VV+AA}$$

B_K NPR with RI/MOM and exceptional momenta

- Calculate four-quark vertex matrix element in Landau gauge.
- Amputate vertex with ensemble averaged unrenormalised propagator, giving $\Lambda_{\mathcal{O}_{VV+AA}}$
- Renormalisation condition: Fix to tree level value at $\mu^2 = p^2$

$$\frac{Z_{VV+AA}}{Z_q^2}\Lambda_{\mathcal{O}_{VV+AA}} = \mathcal{O}^{\mathrm{tree}}_{VV+AA}$$

- Define

$$\begin{aligned} Z_{BK}^{RI/MOM} &= \frac{Z_{VV+AA}}{Z_A^2} \\ &= \left(\frac{Z_q^2}{Z_A^2}\right)\frac{Z_{VV+AA}}{Z_q^2} \end{aligned}$$

B_K NPR with RI/MOM and exceptional momenta

- Calculate four-quark vertex matrix element in Landau gauge.
- Amputate vertex with ensemble averaged unrenormalised propagator, giving $\Lambda_{\mathcal{O}_{VV+AA}}$
- Renormalisation condition: Fix to tree level value at $\mu^2 = p^2$

$$\frac{Z_{VV+AA}}{Z_q^2}\Lambda_{\mathcal{O}_{VV+AA}} = \mathcal{O}^{\mathrm{tree}}_{VV+AA}$$

- Define

$$\begin{aligned} Z_{BK}^{RI/MOM} &= \frac{Z_{VV+AA}}{Z_A^2} \\ &= \left(\frac{Z_q^2}{Z_A^2}\right)\frac{Z_{VV+AA}}{Z_q^2} \end{aligned}$$

- Use $\frac{1}{2}(\Lambda_A + \Lambda_V) \approx \frac{Z_q}{Z_A}$

Method comparison

$\mathbf{24^3 \times 32}$

$\mathbf{32^3 \times 64}$

Method comparison

$16^3 \times 32$

- Use point sources, 4 quark vertex formed at source location.

$32^3 \times 64$

Method comparison

$16^3 \times 32$

- Use point sources, 4 quark vertex formed at source location.
- Average over 4 source locations on 75 configurations on our $m_l = 0.03, 0.02$ and 0.01 ensembles.

$32^3 \times 64$

Method comparison

$16^3 \times 32$

- Use point sources, 4 quark vertex formed at source location.
- Average over 4 source locations on 75 configurations on our $m_l = 0.03, 0.02$ and 0.01 ensembles.
- Momentum applied by applying phase difference between propagator source and sink. Solution can be given arbitrary momentum.

$32^3 \times 64$

Method comparison

$16^3 \times 32$

- Use point sources, 4 quark vertex formed at source location.
- Average over 4 source locations on 75 configurations on our $m_l = 0.03, 0.02$ and 0.01 ensembles.
- Momentum applied by applying phase difference between propagator source and sink. Solution can be given arbitrary momentum.

$32^3 \times 64$

- Use lattice volume sources, vertex formed at propagator sink. (D. Broemmel)

Method comparison

$16^3 \times 32$

- Use point sources, 4 quark vertex formed at source location.
- Average over 4 source locations on 75 configurations on our $m_l = 0.03, 0.02$ and 0.01 ensembles.
- Momentum applied by applying phase difference between propagator source and sink. Solution can be given arbitrary momentum.

$32^3 \times 64$

- Use lattice volume sources, vertex formed at propagator sink. (D. Broemmel)
- Average over all sink locations, lattice volume factor gain over point approach.

Method comparison

$16^3 \times 32$

- Use point sources, 4 quark vertex formed at source location.
- Average over 4 source locations on 75 configurations on our $m_l = 0.03, 0.02$ and 0.01 ensembles.
- Momentum applied by applying phase difference between propagator source and sink. Solution can be given arbitrary momentum.

$32^3 \times 64$

- Use lattice volume sources, vertex formed at propagator sink. (D. Broemmel)
- Average over all sink locations, lattice volume factor gain over point approach.
- Volume source has fixed momentum as phase must be applied to source lattice sites before inversion.

Method comparison

$16^3 \times 32$

- Use point sources, 4 quark vertex formed at source location.
- Average over 4 source locations on 75 configurations on our $m_l = 0.03, 0.02$ and 0.01 ensembles.
- Momentum applied by applying phase difference between propagator source and sink. Solution can be given arbitrary momentum.

$32^3 \times 64$

- Currently calculated 5 independent momenta (10 total) on 10 configurations on our $m_l = 0.006$ and 0.004 ensembles

$Z_{BK}^{RI/MOM}(\mu)$

$16^3 \times 32$

$32^3 \times 64$

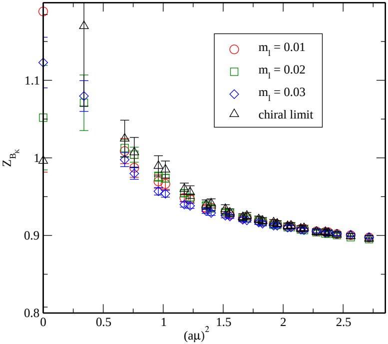

$Z_{BK}^{RI/MOM}(\mu)$

$16^3 \times 32$

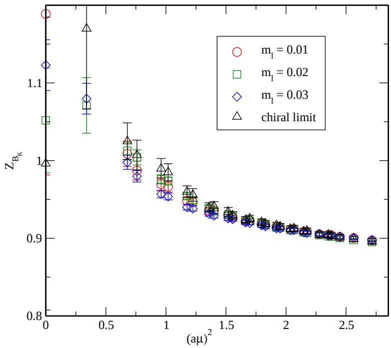

$32^3 \times 64$

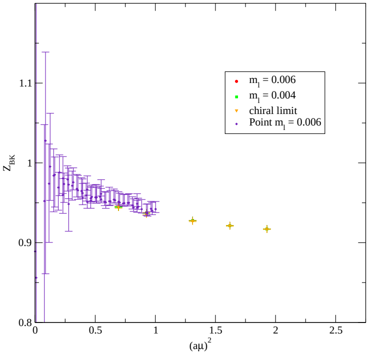

$Z_{BK}^{RI/MOM}(\mu)$

$16^3 \times 32$

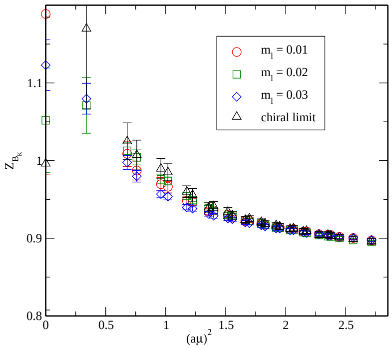

$32^3 \times 64$

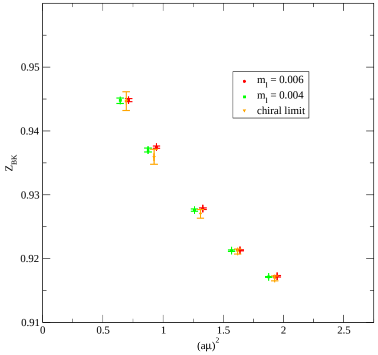

Chiral extrapolation – $32^3 \times 64$

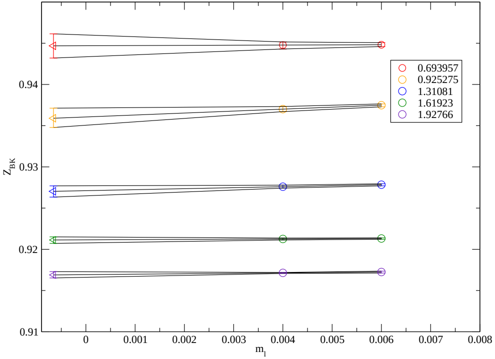

- For each $Z_{BK}(\mu)$, perform a linear chiral extrapolation to $m = -m_{\rm res}$

Chiral extrapolation – $32^3 \times 64$

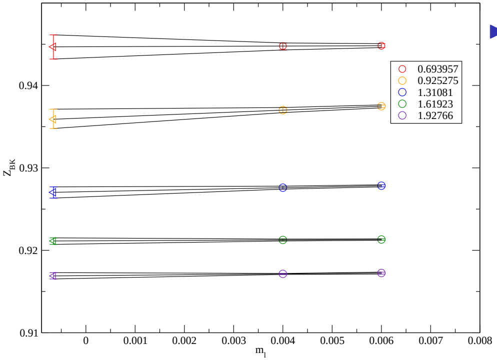

- For each $Z_{BK}(\mu)$, perform a linear chiral extrapolation to $m = -m_{\text{res}}$
- 32^3 lever-arm for extrapolation small compared to extrapolation distance

Chiral extrapolation – $32^3 \times 64$

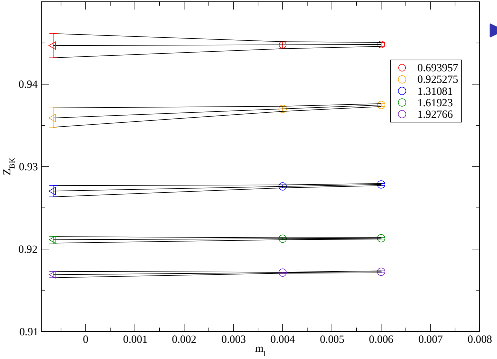

- For each $Z_{BK}(\mu)$, perform a linear chiral extrapolation to $m = -m_{\mathrm{res}}$
- 32^3 lever-arm for extrapolation small compared to extrapolation distance
  $\longrightarrow$ Future: Add $m_l = 0.008$ dataset

Exceptional momenta systematic error

- 32^3 stat errors small compared to systematic error from exceptional momenta.

$32^3 \times 64$

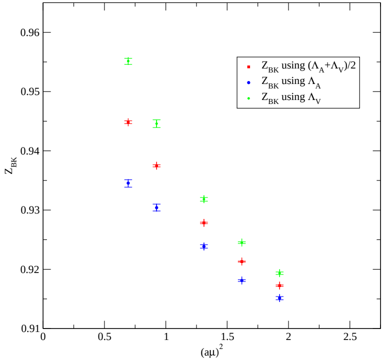

Exceptional momenta systematic error

- 32^3 stat errors small compared to systematic error from exceptional momenta.
- On 24^3 we attributed a 1.5% sys error to this alone.

$32^3 \times 64$

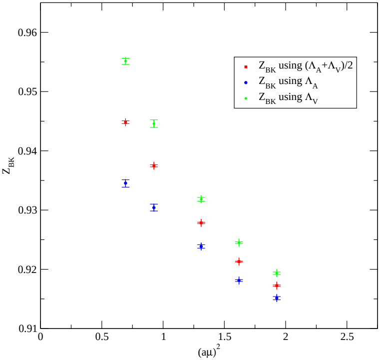

Exceptional momenta systematic error

- 32^3 stat errors small compared to systematic error from exceptional momenta.
- On 24^3 we attributed a 1.5% sys error to this alone.
- Difference greatly reduced by using non-exceptional momentum configuration $p_1 \neq p_2$

$32^3 \times 64$

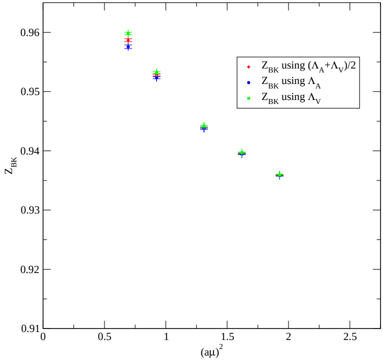

Exceptional momenta systematic error

- 32^3 stat errors small compared to systematic error from exceptional momenta.
- On 24^3 we attributed a 1.5% sys error to this alone.
- Difference greatly reduced by using non-exceptional momentum configuration $p_1 \neq p_2$
- Unfortunately no perturbative calculation available for non-exceptional (Y. Aoki)

$32^3 \times 64$

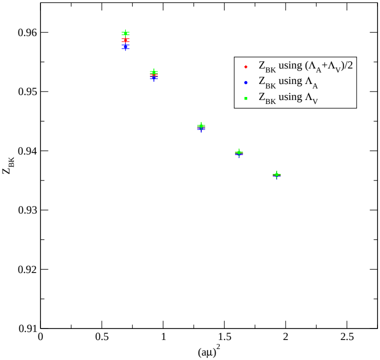

Removal of lattice artefacts

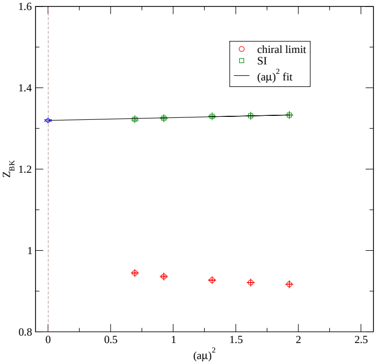

- Divide out perturbative running: Quantity is scale invariant up to lattice artefacts

Removal of lattice artefacts

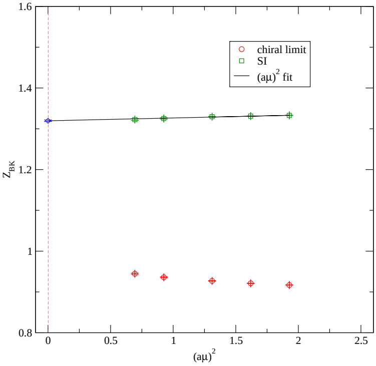

- Divide out perturbative running: Quantity is scale invariant up to lattice artefacts
- Expect quadratic dependence of lattice artefacts on lattice spacing

  $\rightarrow$ fit to form $Z_{BK}^{SI} + B(a\mu)^2$

Extrapolation of Z_{BK}^{SI}

$16^3 \times 32$

$32^3 \times 64$

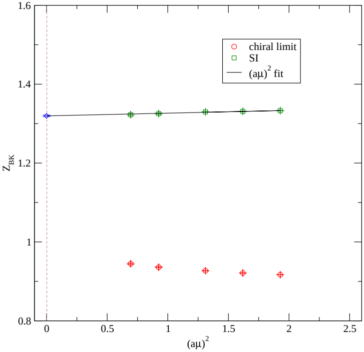

Extrapolation of Z_{BK}^{SI}

$16^3 \times 32$

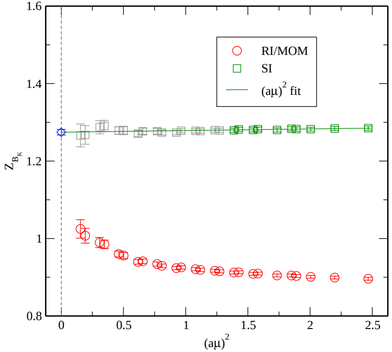

$32^3 \times 64$

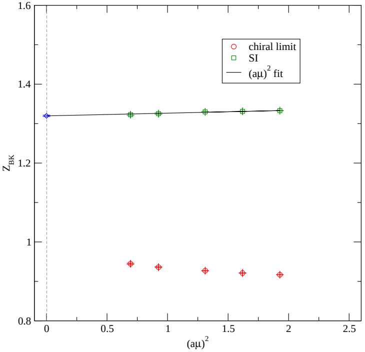

$24^3 \times 64$ result – Aoki *et al* [arXiv:0712.1061]

- Reapply RI/MOM perturbative running to Z_{BK}^{SI} and scale to conventional $\mu = 2$ GeV.

$24^3 \times 64$ result – Aoki *et al* [arXiv:0712.1061]

- Reapply RI/MOM perturbative running to Z_{BK}^{SI} and scale to conventional $\mu = 2$ GeV.
- Apply conversion factor $Z_{BK}^{RI/MOM} \rightarrow Z_{BK}^{\overline{\mathrm{MS}}}$

$24^3 \times 64$ result – Aoki *et al* [arXiv:0712.1061]

- Reapply RI/MOM perturbative running to Z_{BK}^{SI} and scale to conventional $\mu = 2$ GeV.
- Apply conversion factor $Z_{BK}^{RI/MOM} \rightarrow Z_{BK}^{\overline{\mathrm{MS}}}$
- $Z_{BK}^{\overline{\mathrm{MS}}}$ (2 GeV) $= 0.9276 \pm 0.0052(\mathrm{stat}) \pm 0.0220(\mathrm{sys})$.

$24^3 \times 64$ result – Aoki *et al* [arXiv:0712.1061]

- Reapply RI/MOM perturbative running to Z_{BK}^{SI} and scale to conventional $\mu = 2$ GeV.
- Apply conversion factor $Z_{BK}^{RI/MOM} \to Z_{BK}^{\overline{\mathrm{MS}}}$
- $Z_{BK}^{\overline{\mathrm{MS}}}$ (2 GeV) $= 0.9276 \pm 0.0052(\mathrm{stat}) \pm 0.0220(\mathrm{sys})$.
- Sys errors:

$24^3 \times 64$ result – Aoki *et al* [arXiv:0712.1061]

- Reapply RI/MOM perturbative running to Z_{BK}^{SI} and scale to conventional $\mu = 2$ GeV.
- Apply conversion factor $Z_{BK}^{RI/MOM} \to Z_{BK}^{\overline{\mathrm{MS}}}$
- $Z_{BK}^{\overline{\mathrm{MS}}}$ (2 GeV) $= 0.9276 \pm 0.0052(\mathrm{stat}) \pm 0.0220(\mathrm{sys})$.
- Sys errors:
  - $\mathcal{O}(\alpha_s) \Rightarrow 0.0177$ corrections due to truncation of perturbative analysis

$24^3 \times 64$ result – Aoki *et al* [arXiv:0712.1061]

- Reapply RI/MOM perturbative running to Z_{BK}^{SI} and scale to conventional $\mu = 2$ GeV.
- Apply conversion factor $Z_{BK}^{RI/MOM} \to Z_{BK}^{\overline{\mathrm{MS}}}$
- $Z_{BK}^{\overline{\mathrm{MS}}}$ (2 GeV) $= 0.9276 \pm 0.0052(\mathrm{stat}) \pm 0.0220(\mathrm{sys})$.
- Sys errors:
  - $\mathcal{O}(\alpha_s) \Rightarrow 0.0177$ corrections due to truncation of perturbative analysis
  - $\Rightarrow 0.0007$ unphysical strange mass correction

$24^3 \times 64$ result – Aoki *et al* [arXiv:0712.1061]

- Reapply RI/MOM perturbative running to Z_{BK}^{SI} and scale to conventional $\mu = 2$ GeV.
- Apply conversion factor $Z_{BK}^{RI/MOM} \rightarrow Z_{BK}^{\overline{\mathrm{MS}}}$
- $Z_{BK}^{\overline{\mathrm{MS}}}$ (2 GeV) $= 0.9276 \pm 0.0052(\mathrm{stat}) \pm 0.0220(\mathrm{sys})$.
- Sys errors:
  - $\mathcal{O}(\alpha_s) \Rightarrow 0.0177$ corrections due to truncation of perturbative analysis
  - $\Rightarrow 0.0007$ unphysical strange mass correction
  - $\Rightarrow 0.0131$ correction for use of exceptional momenta

$24^3 \times 64$ result – Aoki *et al* [arXiv:0712.1061]

- Reapply RI/MOM perturbative running to Z_{BK}^{SI} and scale to conventional $\mu = 2$ GeV.
- Apply conversion factor $Z_{BK}^{RI/MOM} \rightarrow Z_{BK}^{\overline{\mathrm{MS}}}$
- $Z_{BK}^{\overline{\mathrm{MS}}}$ (2 GeV) $= 0.9276 \pm 0.0052(\mathrm{stat}) \pm 0.0220(\mathrm{sys})$.
- Sys errors:
  - $\mathcal{O}(\alpha_s) \Rightarrow 0.0177$ corrections due to truncation of perturbative analysis
  - $\Rightarrow 0.0007$ unphysical strange mass correction
  - $\Rightarrow 0.0131$ correction for use of exceptional momenta
- Current 32^3 $Z_{BK}^{\overline{\mathrm{MS}}}$ stat error ~ 0.0013.

Conclusions and Outlook

$24^3 \times 64$ final value and 32^3 outlook

- Combining chirally extrapolated B_K with aforementioned Z_{BK} result

$24^3 \times 64$ final value and 32^3 outlook

- Combining chirally extrapolated B_K with aforementioned Z_{BK} result $\quad \rightarrow B_K^{\overline{\mathrm{MS}}}(2\,\mathrm{GeV}) = 0.524(10)_{\mathrm{stat}}(13)_{\mathrm{ren}}(25)_{\mathrm{sys}}$ [arXiv:0804.0473]

$24^3 \times 64$ final value and 32^3 outlook

- Combining chirally extrapolated B_K with aforementioned Z_{BK} result $\quad \rightarrow B_K^{\overline{\mathrm{MS}}}(2\,\mathrm{GeV}) = 0.524(10)_{\mathrm{stat}}(13)_{\mathrm{ren}}(25)_{\mathrm{sys}}$
  [arXiv:0804.0473]
- Improved techniques for 32^3 in use; results expected soon: Watch this space!